International Journal of River Basin Management
Publication details, including instructions for authors and subscription information:
http://www.tandfonline.com/loi/trbm20

Parana River morphodynamics in the context of climate change

Massimo Guerrero [a], Michael Nones [b], Ramiro Saurral [c d], Natalia Montroull [c] & Ricardo N. Szupiany [e]

[a] Hydraulic Laboratory, University of Bologna, Bologna, Italy

[b] Research Center for Constructions - Fluid Dynamics Unit, University of Bologna, via del Lazzaretto 15/5, 40121, Bologna, Italy

[c] Centro de Investigaciones del Mar y la Atmósfera (CIMA/CONICET-UBA), UMI IFAECI/CNRS and Departamento de Ciencias de la Atmósfera y los Océanos (FCEN-UBA), Buenos Aires, Argentina

[d] Universidad de Buenos Aires, Buenos Aires, Argentina

[e] Facultad de Ingeniería y Ciencias Hídricas (FICH), Universidad National del Litoral, Santa Fe, Argentina

Accepted author version posted online: 25 Jul 2013.Published online: 05 Sep 2013.

To cite this article: Massimo Guerrero, Michael Nones, Ramiro Saurral, Natalia Montroull & Ricardo N. Szupiany, International Journal of River Basin Management (2013): Parana River morphodynamics in the context of climate change, International Journal of River Basin Management, DOI: 10.1080/15715124.2013.826234

To link to this article: http://dx.doi.org/10.1080/15715124.2013.826234

Intl. J. River Basin Management iFirst, 2013, 1–15

Research paper

Parana River morphodynamics in the context of climate change

MASSIMO GUERRERO, *Hydraulic Laboratory, University of Bologna, Bologna, Italy*

MICHAEL NONES, *Research Center for Constructions – Fluid Dynamics Unit, University of Bologna, via del Lazzaretto 15/5, 40121, Bologna, Italy. Email: michael.nones@unibo.it (Author for correspondence)*

RAMIRO SAURRAL, *Centro de Investigaciones del Mar y la Atmósfera (CIMA/CONICET-UBA), UMI IFAECI/CNRS and Departamento de Ciencias de la Atmósfera y los Océanos (FCEN-UBA), Buenos Aires, Argentina*; *Universidad de Buenos Aires, Buenos Aires, Argentina*

NATALIA MONTROULL, *Centro de Investigaciones del Mar y la Atmósfera (CIMA/CONICET-UBA), UMI IFAECI/CNRS and Departamento de Ciencias de la Atmósfera y los Océanos (FCEN-UBA), Buenos Aires, Argentina*

RICARDO N. SZUPIANY, *Facultad de Ingenierìa y Ciencias Hìdricas (FICH), Universidad National del Litoral, Santa Fe, Argentina*

ABSTRACT

This paper presents an analysis of the sediment dynamics that takes place at different scales within the Middle and the Lower Parana River in the La Plata Basin. The aim of this study is to provide a multi-disciplinary and multi-scale approach for the prediction of river future morphology in the context of climate change, the intended use of which is the prognosis of river morphodynamics' long-term impact on manmade structures and activities over or near the river. The study is based on three levels of mathematical modelling, with the output of wider-scale models providing the input conditions for more specific ones. Climate models give the input ensemble, i.e. future precipitation and temperature over La Plata Basin. The semi-distributed macro-scale variable infiltration capacity hydrological model simulates the flow discharge time series that are applied to an own-developed 1D morphodynamic model. The 1D model simulates future rate of sediment transport and corresponding bed-level changes at watershed scale and provides the boundary conditions for a 2D model. Therefore, streamflow divagations at channel scale are simulated by means of the MIKE21C code developed by the Danish Hydraulic Institute. The analysis indicates a rather low sensitivity of the Parana River bed profile, i.e. 1D morphology, to the increase predicted in flow discharge, whereas the streamflow appreciably divagates. In particular, surpassing an upper bound in the most frequent discharge appears effective in driving the actual bifurcated morphology into a meandering-multithread configuration.

Keywords: Parana River; climate change impact; sediment transport; morphodynamics; river morphology

1 Introduction

The Parana River represents an important resource for the South America region of La Plata Basin, which gathers parts of five countries (Argentina, Bolivia, Brazil, Paraguay and Uruguay) and whose economy strongly depends on water resources: hydropower production, goods trading throughout the Parana−Paraguay waterway and flood safety policy. The water-sediment dynamics at the Parana River has been studied by different authors aiming to understand and characterize the interrelationship between the climate-hydrology, the fluvial hydraulics and the resulting morphology that in turn affects the water resources. These studies separately focus on different aspects ranging from the macroscale of climate variability at La Plata Basin to the microscale of settling and swiped particles within water fluxes.

The twentieth-century climate of La Plata Basin was subdivided into three periods in previous studies, as in Garcia and Vargas (1998) and Garcia *et al*. (2002), with a dry period of 40 years in the middle and wet periods at the starting and closure of the century. In particular, precipitation had the same behaviour in the upper and lower basin, therefore giving rise to the same streamflow tendency changes within the century. A near-30-year-long period can be argued in the stream flow variability

Received 19 February 2013. Accepted 15 July 2013.

ISSN 1571-5124 print/ISSN 1814-2060 online
http://dx.doi.org/10.1080/15715124.2013.826234
http://www.tandfonline.com

(i.e. interdecadal variability) that is correlated to climate indices (Maciel *et al*. 2010). Other evidences suggest that part of the increase in discharge starting from 1970 to 1971 was due to land-use change in the Brazilian area of the basin, beginning in 1968 (Garcia *et al*. 2002). In addition, Doyle and Barros (2011) showed that part of the increase in runoff was caused by land-use change in the north, by climate variability in the south and by both in the middle part of the basin.

Amsler *et al*. (2005) quantitatively analysed how the streamflow interdecadal variation affected the channel morphology of the Parana River in its middle reach during the twentieth century. Castro *et al*. (2007) carried out a similar study for a 50 km-long reach at the Lower Parana between Puerto San Martin and Alvear (near Rosario City). Amsler *et al*. (2005) related the climate interdecadal variability to the effective discharge (i.e. the discharge value most effectively modifying the morphology) variation and, as a consequence, to river morphological changes. In particular, the dry midst of the century (1930–1970) was characterized by low effective discharge that promoted a decrease in width, braided index, thalweg sinuosity, width to depth ratio and channel volume, with the opposite pattern found in the beginning and end of the century. In other words, for the Middle Parana, the dry period has accomplished a reduction in sediment transport and river channel planimetric dimensions, while wet periods, on the contrary, have increased sediment transport and river channel width, giving rise to islands formation within it. The Lower Parana morphodynamics is not straightforward correlated to hydrological variability as much as the Middle Parana. In particular, historical cartography of the reach between San Martin and Rosario bears out a continuous and progressive oversimplification of the river channel planimetric morphology towards a lower width to depth ratio. In the last part of the century, since 1970, the river channel did not recover the extremely braided morphology that characterized the beginning of the century, on the contrary exacerbating the midst century morphodynamic processes. This occurrence is not easily justified by hydrological interdecadal variability; therefore the authors found additional reasons in the alluvial plane morphology that starting from San Martin up to the La Plata River enlarges and decreases in slope. This morphology constraint together with increased effective discharge during the last part of the century would have produced sediment deposition at secondary reaches and therefore the streamflow gathering in a single straight and deep reach.

Amsler *et al*. (2007) studied in-depth the main channel and floodplain interrelationship at the middle reach of the Parana River. In that study it has been concluded that, on average, $130-135\times10^6$ t/year of sediments are transported through the middle reach, 80% of which is made up of wash load, i.e. silt and clay, almost completely supplied from the upstream subbasins of the Bermejo, a tributary of the Paraguay River flowing from the Bolivian Andes. The rest is fine-medium sand forming the Parana River bed and suspended within the water column: suspended load for the 18%, or rolling and jumping near the bed, i.e. bed load, for the 2%. It is finally argued that clay and silt coming from the Bermejo River consistently affect the floodplain level through the wash load sedimentation that occurs with a stage near the bankfull level, whereas the river channel morphology is modified by the streamflow transport of fine-medium sand.

In such a large and complex system as the Parana – Paraguay River, the prediction of future morphology trends due to climate-hydrology changes is challenging because of the many processes equally concurring, and within a wide range of temporal and spatial scales. Moreover, the management of sediment appears as a key policy to preserve the water resources of the La Plata Basin, which needs to be sustained and driven with reliable prediction of future sediment rate and morphodynamics trends. Different mathematical models were applied in this study to simulate the main known mechanisms that concur with the formation of the Parana River morphology as pointed out in the mentioned literature. The specific objective of this study was therefore to assemble mathematical models from neighbouring subjects within climatology, hydrology and sedimentology disciplines and to develop a simplified tool for sediment management for the Parana River. The intended use of this tool is the prognosis of river morphodynamics' long-term impact on manmade structures and activities over or nearby the river (e.g. the inner navigation within the Parana – Paraguay waterway).

Outputs from four regional climate models (RCMs) were used to assess present and future climate precipitation scenarios with simulations covering much of the twenty-first century: PROMES (UCLM, Spain) covering a continuous run from 1991 to 2098, RCA (SMHI, Sweden) from 1981 to 2100, RegCM3 (USP, Brazil) having information in periods 1981–2048 and 2071–2090, and LMDZ (IPSL, France) with information in periods 1991–2048 and 2071–2100. All RCMs had spatial resolutions of $0.5^\circ\times0.5^\circ$. These climate model simulations were developed under the research project 'A Europe-South America Network for Climate Change Assessment and Impact Studies in La Plata Basin' (CLARIS-LPB) and forced with daily data from global climate models (GCMs). More information on this dataset can be obtained in Saurral *et al*. (2013).

The La Plata Basin surface hydrology was modelled using the variable infiltration capacity macroscale semi-distributed model (VIC; Liang *et al*. 1994, 1996, Nijssen *et al*. 1997) to transform precipitation into rivers runoff at monthly scale. The utility of this model for hydrological studies is proved in many basins worldwide, including La Plata basin itself (Su and Lettenmaier 2009, Saurral 2010, Montroull *et al*. 2012).

The hydrological model gave the inflow conditions for the following simulations at yearly time scale that illustrate the river morphology sensitivity to future scenarios driven by the four RCMs.

The middle-lower reach of the Parana River was represented with a simplified cross-sections scheme for the simulation of hydraulic characteristic, i.e. water depth and velocity changes along the river's longitudinal axis, i.e. 1D model. The simulated

hydraulics was then applied to a 1D morphodynamics model to assess bed sediment transport (suspended and bed loads) and long-term morphology (100 years) in terms of cross-section active width and bed slope changes spanning the period 1991–2098 for two scenarios, and the periods 1991–2048 for the other two, in all the cases simulating yearly average discharges. The 1D hydro-morphodynamics model also gave the boundary conditions for the following simulation at a more detailed scale. In fact, the shallow water approximation was assumed to simulate at yearly time scale the water and bed sediment fluxes in the 25-km-long and 4-km-wide section of the Lower Parana between San Martin and Rosario that presents two junctions and two bifurcations. This Lower Parana section is a significant case study for the characterization of future changes in the typical sequence of nodal sections and islands that describe the Lower Parana; furthermore, it is the most important stretch of the navigation channel because the principal ports are located there. Albeit with a simplified approach, aimed to speed up the computation, the river channel divagation and islands dynamics over the depth averaged plane, i.e. the 2D dynamics, were therefore simulated spanning the calibration period 1954–1976 and the 29 years (i.e. 2010–2038) of the four future scenarios. Given the historical maps and morphological data reported in Castro *et al*. (2007), several simulations of the calibration period were applied to analyse the sensitivity of the resulting morphology to model parameters, also accounting for the influence of the inactive portion of the river in terms of different hydraulic roughness.

This paper is organized as follows: Section 2 presents the La Plata Basin and its main tributary, the Parana River, especially focusing on the 1D simulated middle and lower reaches and on the 25-km-long section of the 2D case study. Detailed descriptions of the applied models can be found in Su *et al*. (2009) for VIC, in Nones *et al*. (2012b) for the 1D hydro-morphodynamic model, and in DHI (2002), Olesen (1987) and Talmon (1992) for the 2D model. Only the most relevant features to the simulations of future scenarios are reported in Section 3 for each model, also including the performed sensitivity analysis to calibrate the 2D model. Section 4 gives the results of the performed simulations of future scenarios. Both Sections 3 and 4 are divided into three subsections reporting: (1) hydrology, (2) 1D morphodynamics and (3) 2D morphodynamics. The applied climate scenarios are briefly introduced in Subsection 4.1 and more details can be found in Saurral *et al*. (2013). Section 5 elucidates the effectiveness of simulated processes in changing river morphology. A set of conclusions, reported in Section 6, emphasize the usefulness of the carried out study giving a simplified tool for predicting the future morphology trends in the light of climate change.

2 The study site

The Parana River is the main tributary of the 3.2×10^6 km^2 large Plata Basin that includes parts of Brazil, Bolivia, Paraguay, Uruguay and Argentina. Figure 1 shows the Plata Basin and the entire Parana River (Figure 1(a)), the 1D-simulated reach from Corrientes to Villa Constitución, near the delta (Figure 1(b)) and the 2D-simulated 25-km-long and 4-km-wide section that is located in the Lower Parana between the cities of San Martín and Rosario, Argentina (Figure 1(c)).

The Parana River is one of the largest rivers in the world and has a drainage basin of 2.3×10^6 km^2 conveying waters into the south-west Atlantic Ocean bordering Buenos Aires, Argentina (Figure 1(a)). From Corrientes to the river delta, the mean annual discharge is approximately 12,000–15,000 m^3/s, the water surface slope is of the order of 10^{-5} and the average total sediment transport (wash load included) is approximately $130–135 \times 10^6$ t/year (Amsler *et al*. 2007) at the Middle Parana. The channel bed is composed largely of well-sorted sand with a mean grain size of approximately 200–300 μm. The mean channel widths and depths range are 600–2500 m and 5–16 m, respectively. A succession of nodal sections, such as expansion bifurcations and confluence contractions, characterize the river channel planform. The river represents one of the most important inner navigation ways of the world, with approximately 100 million tons of cargo transported per year (Escalante 2008).

The 1D-simulated sections correspond to the Middle and Lower Parana (two reaches of the Parana approximately 900 km long in total) that play a key role in the sediment transport processes and associated morphodynamics. In fact, clay and silt materials (80% of solid discharge) coming from the Bermejo River (an east tributary of the Paraguay River) are mainly transported as wash load. During flood periods, they are transported through the delta and the wetlands in up to 30-km-wide plains, while the remaining 20% (i.e. $20–25 \times 10^6$ t/year) is fine sand from the river bed that is transported as bed and suspended load and modifies the channel morphology (i.e. bed slope, channel sinuosity and nodal sections). As visible in Figure 1(b), during the analysis the river cross-sections were named by using the distances of the navigation way from the city of Buenos Aires.

The 2D-simulated section is a significant case study for the characterization of future changes in the typical sequence of nodal sections and islands at the Lower Parana; furthermore it is the most important stretch of the navigation channel because the inward sailing of the oceanic boats ends there.

3 Mathematical models

3.1 *Hydrological model*

The VIC model (Liang *et al*. 1994, 1996, Nijssen *et al*. 1997) is a distributed grid-based land surface scheme capable of solving both water and energy balances on a grid mesh. The main components of the surface hydrological cycle are simulated using a mosaic-like representation of land cover and a subgrid

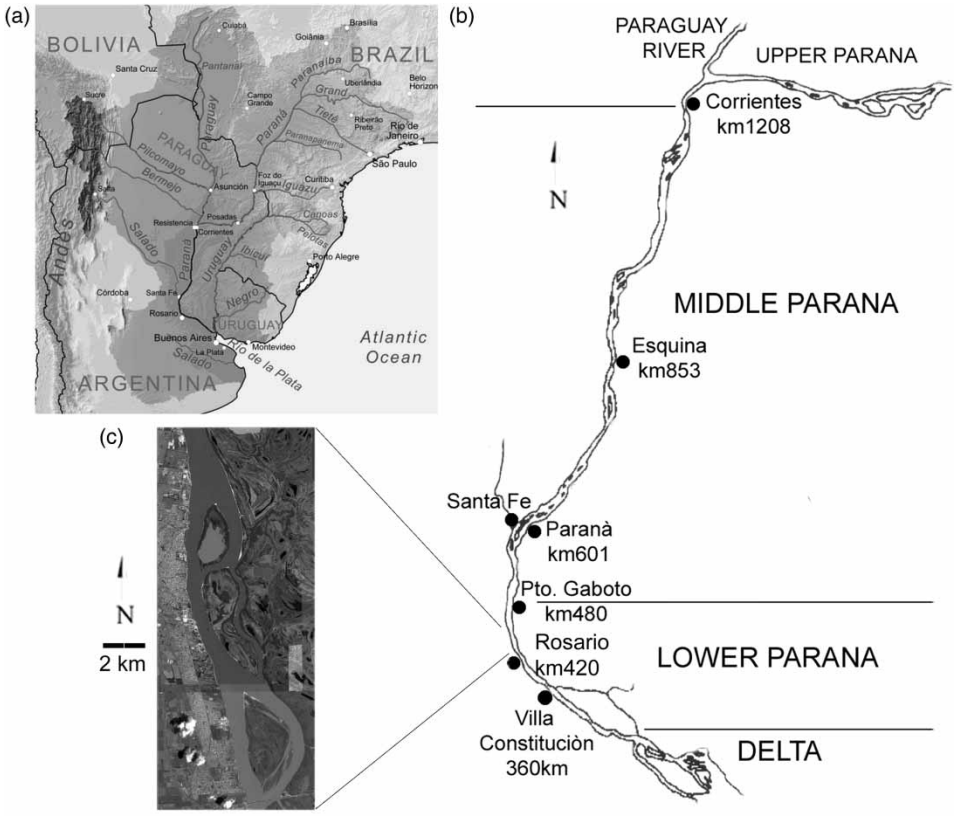

Figure 1 (a) La Plata Basin; (b) the 1D-simulated section corresponding to the Middle and Lower Parana; (c) the 2D-simulated section at the Lower Parana.

parameterization for infiltration. It requires information on soil texture, topography and vegetation. Soil data were derived from the 5-min Global Soil Data Task dataset from the Distributed Active Archive Center (2000) and vegetation information was obtained from the University of Maryland's 1-km Global Land Cover product (Hansen *et al*. 2000). Topography information to derive streamflow data from surface and sub-surface runoff at every grid point was obtained from the Global Land One-Kilometer Base Elevation (GLOBE) dataset developed by Hastings *et al*. (1999). In this paper, meteorological data used to force the model consisted of daily minimum and maximum temperature and daily precipitation from past century records and future scenarios. Spatial resolution for VIC was selected at 1/8 degree, so all meteorological data were re-gridded to that resolution before using it to force the hydrological model.

3.2 *1D morphodynamic model*

An own-developed model, able to describe the hydrological and morphological variations at watershed scale (Di Silvio and Peviani 1989), was applied to analyse the longitudinal evolution of the Parana River. This model, i.e. the Local Uniform Flow Morphodynamic (LUFM) model, is based on various simplifications, but the most important one is the Local Uniform Flow (LUF) hypothesis, under which the uniform flow is assumed to be fulfilled on average at the appropriate length (morphological box) and duration (evolution window) scales (Fasolato *et al*. 2011).

The Parana River was divided into 10 morphological boxes, having a length of about 80 km for each one, on the basis of assessed values for the Froude number of the river. The Engelund and Hansen formula (1969) was applied for computing the transport rate of sediment from the river bed (i.e. bed load plus suspended load, wash load not included; hereinafter simply referred as sediment transport) for each morphological box.

In the present work, the LUFM model is coupled to a simplified description of the river cross-section evolution, necessary for computing the active cross-section width as a function of the river discharge, rather than assuming a fixed width of the river bed. The river cross-section evolution was simulated at yearly time scale, which is shorter than the evolution window (having the duration on the order of some years). In fact aiming to reproduce the interdecadal variability effectiveness in modifying the river morphology, the cross-section width changes were correlated to the relative short time scale of the forcing hydrology, while the longitudinal evolution of the river profile was computed with a longer time step, in order to describe its long-term variation.

The active cross-section is defined as the river channel width that conveys the annual sediment transport and it is therefore applied to compute the sediment transport at each morphological box.

For many rivers, recent cross-sections (including the vegetation cover) of the entire water course are not available from topographic surveys, and in such a case the applied synthetic approach is particularly helpful. In fact, a given cross-section is defined by the statistical distribution of its width as a function of the corresponding statistical distribution of the river discharge (Nones 2011). Wherever possible, as in more recent years, this correlation can be obtained from satellite images of wetted and vegetated areas, which indicate the changing morphology characterizing the river. For this study, the Landsat 7 images (USGS database) related to the period 2000–2010 were used as an indicator of the Parana River's geometry. A detailed description of the calibration procedure at the Parana River of the LUFM model is reported in Nones (2011).

3.3 *2D morphodynamic model*

A mathematical model of the water-sediment fluxes, bed morphology and sediment size variation in curved alluvial rivers was applied to the 25-km-long section at the Lower Parana (Figure 2). The model was written by DHI in the MIKE21C 2D shallow water code. This model solves two-dimensional Navier–Stokes equations for the liquid phase and the continuity equation for the sediment on a curvilinear grid using a finite difference scheme; a detailed description of the model can be found in DHI (2002), Olesen (1987) and Talmon (1992). Only the model's fundamental features that are relevant to the morphodynamic calibration in this study are reported in the paper. In particular, the hydraulic and morphological modules run with different time steps, each one fitted to the rate of the represented process, the morphodynamics being several order slower than the propagation of free surface perturbation. Given these differences, the hydraulics was maintained quasi-steady within an individual morphological step (i.e. the hydraulic time step is scaled to the morphological time step) that yields the same marching time for the hydro- and morpho-dynamic computations. Hence, the modules run interactively to account for reciprocal feedback between morphology and water-sediment fluxes. These features make the model particularly fitted to the representation of slow processes such as the long-term morphodynamics of large rivers.

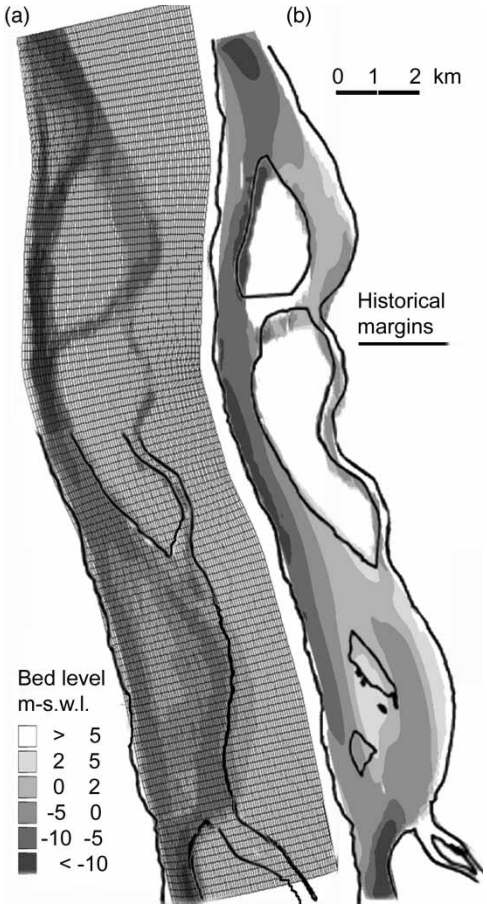

Figure 2 (a) 2D model computational grid over the initial (1954) reconstructed bathymetry with the corresponding historical margins; (b) the 1976 margins over the resulting morphology from the calibration period (1954–1976).

In the case study, the hydraulic and morphological time steps were fixed to 5 s and 6 h, respectively; shorter values up to 2 s and 3 h, respectively, were also tested and did not lead to relevant changes in the simulation results. The inflow and outflow conditions at the boundaries were represented by means of yearly averaged values (i.e. yearly time scale): this is consistent with the quasi-steady approach and with the objective to simulate long-term morphodynamics' trend that is related to inter-decadal variability of climate.

The curvilinear grid is intended for the detailed simulation of river and channels where an accurate description of bank lines is required. In the case study, channel margins were roughly represented from historical maps and the bank lines erosion and islands formation were qualitatively simulated aiming to reproduce secondary channels divagation. In fact, the lateral erosion rate is proportional to the bed erosion and sediment transport rate near margins, but the failure mechanism of river margins is not directly represented in the model. Therefore, although the accurate representation of bank lines was not a main goal of this study, the results' sensitivity to different grid shape and mesh size was preliminary tested (Guerrero and Lamberti 2013). Finally, the selected grid (Figure 2(a)) follows the low-curvature orientation of the right margin that, in agreement with observed margins (Figure 3), was considered as a morphological constraint for the long-term simulations performed. The transversal and longitudinal mesh sizes were fixed to 200 and 60 meters on average over the computation domain, respectively, and further halving these sizes gave rise to not appreciable changes in the resulting morphology.

A wet and dry algorithm allows the water stage to change significantly during simulations (except near the boundary condition locations). Boundary conditions at the downstream water level, and the upstream flow discharge and sediment transport, were derived from the 1D model. The Engelund and Hansen formula (1969) for estimating the sediment transport was also

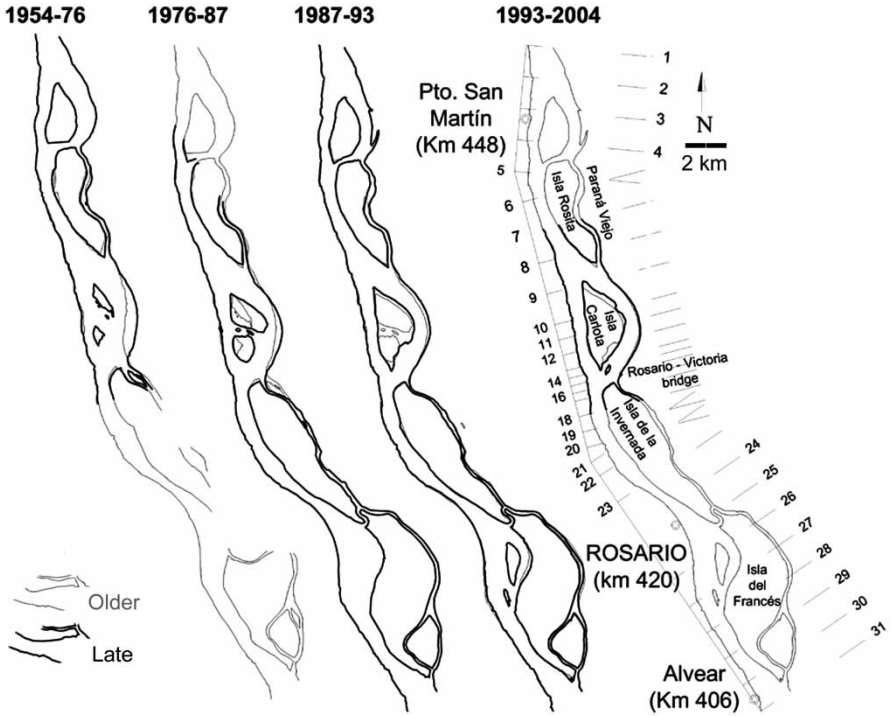

Figure 3 Parana River historical margins between San Martin and Rosario (courtesy of Instituto Nacional del Agua, Buenos Aires).

applied in the 2D model domain; this formula accounts for a simplified single-fraction and isotropic sand distribution with a mean particle size of 250 μm. The assessment of loads was subdivided with 90% of sediment transported in suspension and the remaining 10% of sediment transported as bed load in agreement with Amsler *et al*. (2007). In this application, the wash load was not simulated, because it mainly affects the floodplain, while the river channel morphological changes are most related to the transport of the channel bed material (simulated here). Boundary conditions from the 1D model and the Engelund and Hansen formula applicability to the case study were verified in Guerrero and Lamberti (2013).

Bed roughness can be defined either by means of the total Chézy, χ in $m^{1/2}/s$, or the Gauckler−Strickler, k in $m^{1/3}/s$, parameter and as a constant value or by a power law of the water depth, h. The roughness dependence on water depth was tested with the objective to map an increased resistance to water flow over islands and alluvial plane (i.e. for low-depth regions) which in turn affects the lateral erosion, or a fixed Gauckler−Strickler value of 36 $m^{1/3}/s$ was assumed in agreement with the observed alluvial resistance (Guerrero and Lamberti 2013).

The model accounts for the secondary flow, which is the flow component perpendicular to the primary longitudinal direction, and the effect of the river bed slope on the sediment transport direction, and simulates island and bank erosion-deposition. These features make the model quasi-3D, but introduce parameters in the equation of continuity for the sediment that require an accurate calibration. In particular, the sediment transport direction in the model mainly depends on two parameters as discussed in Guerrero *et al*. (2013) and Guerrero and Lamberti (2012): (1) α that represents the secondary flow diverting sediment loads from the mean flux direction, producing a lateral deposition which increases the side-slope of the channel cross-section and (2) G that simulates the counteracting effect of gravitational sliding which levels the channel cross-section. In addition, bank-island erosion was assumed to be proportional to the bed erosion by means of the model parameter α_E. The eroded material is assumed to be the same as the sediment of the river bed and is therefore included in the continuity equation for sediments.

The calibration of the 2D model is reported in Guerrero and Lamberti (2013), where the Gauckler−Strickler parameter values and the Engelund and Hansen formula were verified against field data (Guerrero *et al*. 2011, 2012), and historical and analytical results by means of steady-state simulations over a fixed morphology.

The result of a further analysis of the morphodynamic module performance is herein reported. The inflow and outflow conditions at boundaries were supplied by the 1D model simulation of the twentieth century; in addition the left channel was closed at the downstream boundary in agreement with the observed margins modification passing from 1954 to 1976 (Figure 2(a) and 2(b)).

As can be seen from historical margins in Figure 3, the formation process of the Carlota Island took place at the simulated downstream sub-section (cross-sections from 8 to 14) and later yielded the thalweg diversion from the left-meandered path to the raising straight and deep channel at the right bank, bordering the Carlota Island (Figure 3). In this figure, the river cross-sections were labelled from 1 to 31.

The morphological changes' sensitivity to model parameters, i.e. α, G and α_E, and to the flow-resistance law was analysed by simulating the period 1954–1976. This period is most significant in terms of occurred morphodynamics at the Carlota Island driven by the increase of the yearly average discharge that most affects the morphology (i.e. the effective discharge). This increase, computed by means of yearly averaged discharges (Nones *et al*. 2012b), was from 13,000 to 17,000 m^3/s passing from the 1950s to the 1970s.

Table 1 summarizes the assumed values for the morphological parameters, and the resulting mean water depth, H, and wetted volume, V, on 1976. H is the average of the domain water depths on simulation end (1976) and V is the water volume integral of the corresponding wetted cells. The same table reports H and V values assumed for starting (1954) bathymetry. These values were compared to historical observations as retrieved from Castro *et al*. (2007), with respect to 1950 and 1979. In this case the authors estimated H and V from the reference level of Rosario's gauge station (3.04 m swl) that is around 8–10 m above the actual minimum bed level. Figure 2(b) shows the 1976 resulting morphology for simulation 9 and Figure 2(a) the initial bathymetry as reconstructed from 1954 margins and corresponding historical data (Castro *et al*. 2007) reported in Table 1. Given the objective of simulating the Island Carlota's formation, notice that only the most important past features were accounted for in the initial bathymetry, i.e. the 2009 bathymetry (Guerrero and Lamberti 2013) from cross-sections 8 to 14 in Figure 3 was recasted to 1954 morphology, whereas the remaining part, including island and alluvial plane level, was maintained similar to the 2009 morphology. In fact, the margins of the upstream and downstream parts did not change significantly passing from 1954 to the present (Figure 3).

Albeit the applied oversimplifications, the Carlota Island's formation was pretty satisfactorily simulated when assuming Eq. 1 to map the flow resistance:

$$\chi = 10 \cdot h^{0.67}, \tag{1}$$

where water depth is expressed in meters to asses the Chézy parameter in $m^{1/2}/s$. In those cases the resulting mean water depth, H, and wetted volume, V, appeared better consistent with observed value in 1979 (Castro *et al*. 2007). Figure 4 reports the assumed flow resistance law for different simulations; notice that the Gauckler−Strickler parameter value equal to 36 $m^{1/3}/s$ corresponds to Eq. 2 as Chézy parameter:

$$\chi = 36 \cdot h^{1/6}. \tag{2}$$

Equation 1 exacerbates the resistance to flow at low-water-depth regions with respect to Eq. 2. In some way, this increased resistance simulates the effectiveness of Parana's floodplain and islands in deviating the streamflow. In fact, the planimetric distribution of roughness simulated by Eq. 1 reduces the lateral erosions at island and shore margins finally affecting the resulting morphology. On the other hand, Eq. 1 also exacerbates flow resistance changes in the river channel because of discharge modification which may be related to alluvial roughness. Indeed, the main reasons to flow resistance in the Parana River channels are grain- and form-roughness which in the calibration performed by Guerrero and Lamberti (2013) fixed the Gauckler−Strickler parameter value equal to 36 $m^{1/3}/s$. Therefore, the deviation from 36 m^3/s (i.e. Eq. 1) is only intended to surrogate the resistance to lateral erosion at low-depth area nearby the margin lines.

Table 1 Observed data and 2D model parameters' values and results in 1976.

Observed data					H (m)	V (10^6 $m^{3)}$	Year
Castro *et al*. (2007)					5.18	95.41	1950
					6.21	91.65	1979
Starting bathymetry					5.93	89.76	1954
Simulation	G	α	α_E	Flow-resistance law	H (m)	V (10^6 m^3)	Inversion year
sim. 1	2	0.5	30	$k = 36\ m^{1/3}/s$	9.06	89.85	1960
sim. 2	1	0.5	30	$k = 36\ m^{1/3}/s$	9.15	92.48	1964
sim. 3	3	0.5	30	$k = 36\ m^{1/3}/s$	8.52	80.09	1965
sim. 4	3	0.5	30	$\chi = 10 \cdot h^{0.67}$	7.83	75.67	1967
sim. 5	2	0.0	30	$k = 36\ m^{1/3}/s$	8.52	78.16	1971
sim. 6	3	0.0	30	$k = 36\ m^{1/3}/s$	8.39	75.80	1972
sim. 7	2	0.5	10	$k = 36\ m^{1/3}/s$	8.89	84.89	1967
sim. 8	2	0.5	50	$k = 36\ m^{1/3}/s$	9.07	87.85	1965
sim. 9	3	0.0	10	$\chi = 10 \cdot h^{0.67}$	7.69	68.29	1968
sim. 10	3	0.0	10	$\chi = 5 \cdot h^{0.75}$	7.74	72.18	1966
sim. 11	3	0.0	10	$\chi = 20 \cdot h^{0.42}$	8.10	74.93	1970
sim. 12	3	0.0	50	$\chi = 10 \cdot h^{0.67}$	7.52	67.72	1972

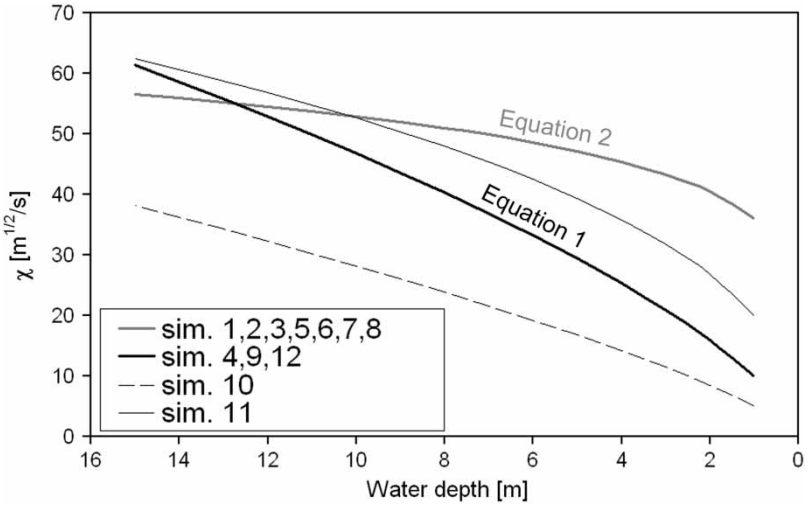

Figure 4 Chézy − water depth relations applied to map the flow resistance in the 2D model.

Table 1 also reports the resulting starting time of flow divagation from the left-meandering path to the raising straight channel bordered by the river right margin at the downstream subsection. The historical margins sequence reported in Castro *et al*. (2007) shows that the island formation in the period 1947–1968 anticipated the main channel switching to the right side in the period 1992–2005. This delay was better represented in runs 9 and 12, which, to some degree, simulate the observed progressive deposition at the entrance of the left branch due to the reduced slope driven by the increasing amplitude of this meandering branch. In fact, in runs 9 and 12, the effects of sediment sliding and lateral erosion (i.e. larger G and α_E parameters) combine to sediment deposition in the meandering branch, while the helical flow effectiveness in deepening the meandering channel is limited by lower α. Finally, in simulation 9, the Carlota Island is better located with respect to observed margins (Figure 2(b)); hence the corresponding parameters were applied to the following scenarios simulations.

4 Scenarios results

4.1 *Hydrological simulations*

Although the CLARIS-LPB project developed a set of climate simulations from seven RCMs, a subset of four of them was selected for hydrological assessment after analysing the ability of all the RCMs to simulate the main present climate features. This includes an analysis of the skill to simulate the mean and standard deviation fields of temperature and precipitation as well as their seasonal cycles. Corrections were applied to the four selected RCMs to remove systematic biases on temperature and precipitation before using them to force the hydrological model (see Saurral *et al*. 2013 for more details).

Monthly discharge time series were derived from the VIC model forced by the RCMs data for selected closing points and observed data in the case of the twentieth century. Figure 5(a) shows the histograms of assessed monthly discharges (covering the twentieth century and much of the twenty-first starting from 1981) at the Parana River in Corrientes, where a relatively large dispersion can be seen among the different RCMs and a general trend towards an increase in the frequency of large discharges with respect to the twentieth-century results. In fact, the RegCM3 predicts a marked shift in the mean value, with little change in the variability/standard deviation, while the other scenarios are characterized by a decrease in the frequency of the most frequent value and an increase in the variance (i.e. the distributions are flatter and more spread out). Depending on the scenario, future time series of monthly discharge are characterized with a larger mean value and variability with respect to the past century.

The yearly averaged discharges applied to the 1D morphodynamic model are reported in Figure 5(b) for the past century together with the corresponding moving average over a 10-year basis that is also plotted for the data from different RCMs. Yearly averaging yields a reduction of about 10,000 m^3/s in maximum discharges on average with regards to monthly values of the past century, but the interdecadal variability is not filtered out as can be seen from the moving average variation. Moving averages of the RCMs data set clearly show the general trend towards larger discharges with respect to the twentieth-century values with the RegCM3 giving the larger deviations in the matching period at the turn of two centuries. In addition, the RCA and PROMES noticeably deviate in the far future (the former yielding largest discharges), while LMDZ is characterized with high-amplitude oscillations when compared to RegCM3.

4.2 *1D morphodynamic simulations*

The simulations performed by the LUFM model provided the 1D evolution of the river with a one-year step in terms of bed profile, bottom shear stress, active river width, flow velocity and water

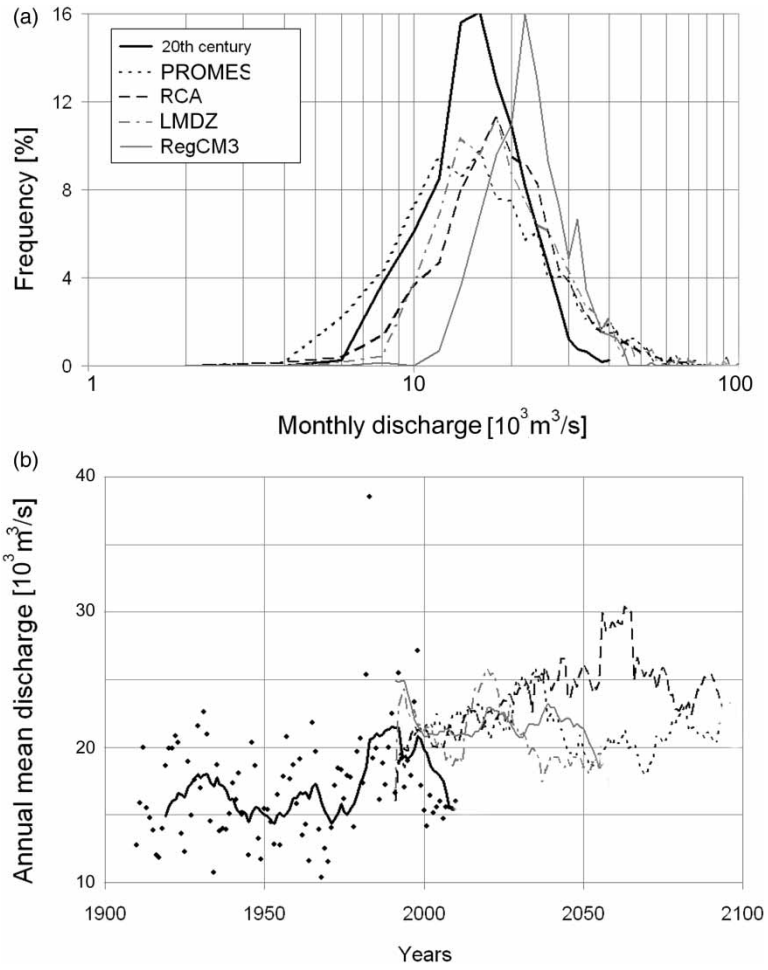

Figure 5 Twentieth-century and future discharges at the Parana River downstream of Corrientes: (a) distributions of monthly discharge; (b) yearly averaged values (dots, only for the twentieth century) and moving averages on a 10-year basis.

level spanning the period 1991–2098 for two scenarios, and the period 1991–2048 for the other two. The model gave very similar longitudinal evolutions of the river, although with hydrological differences: the Lower Parana appears quite stable, with slight aggradation in the order of 10^{-4} m/year, i.e. some centimetres in one century; in addition, a deposition of 10^{-3} m/year resulted in the upper part of the Middle Parana (between 1100 and 800 km of the navigation way) and a slight erosion in the lower part of the Middle Parana (between 800 and 500 km).

The 1D morphology stability of the Parana River, regardless of the applied scenarios, is reflected also in terms of resulting values of water and bed slopes, river width and sediment transport rate; in fact the latter two collapse on the same function of flow discharge (Figure 6(a)). In the Lower Parana, the active channel width varied between 1.7 and 2.7 km, while the sediment transport had a range of $10-50\times10^{6}$ t/year for changing discharge within the interval of 10,000–30,000 m^3/s. The water level and slope varied between 7 and 14 m (Figure 6(b)) and in the $2.2-3.5\times10^{-5}$ range, respectively, for the same reach and discharges. These values agree pretty well with Castro *et al.*'s (2007) observations, though deviations reflect the 1D model limitations in reproducing planimetric change of the active channel morphology and the hydrology averaging inherited from the yearly time scale applied.

Functions of active-channel width, sediment transport rate and water level derived from the 1D model results in Figure 6(a) and 6(b) were used as upstream and downstream boundary conditions, respectively, in the 2D model.

The effective discharge is the flow that cumulates most of the channel bed sediments' transport (Biedenharn *et al*. 1999), i.e. following the Schaffernak approach (Garde and Ranga Raju 1977), it is detected by the maximal product of the interval frequencies and the solid discharges occurring in the intervals as assessed for the corresponding hydrological conditions. Although the simulations were forced with time series of yearly averaged discharge, the 1D model results were also applied to assess the effective discharge and its variability at the Lower Parana within the simulated periods, i.e. the future scenarios and the twentieth century. In this case frequencies were assessed on the basis of 2000-m^3/s-spaced classes spanning the yearly averaged discharges within the simulation periods.

The resulting values were used for a synthetic description of the scenarios with regards to the 1D and 2D simulated periods as reported in Table 2. Figure 7 reports frequency-solid discharge

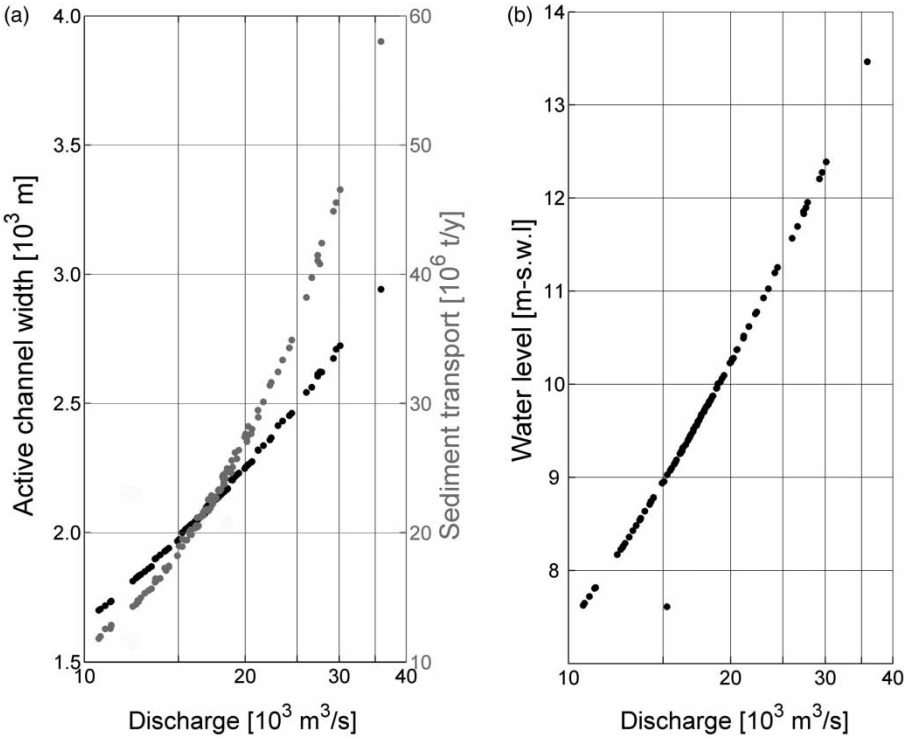

Figure 6 2D model boundary conditions from the 1D model results at the Lower Parana: (a) discharge-sediment transport rate and discharge − active width relations at the upstream boundary; (b) discharge − water level relation.

products, i.e. sediment volumes per year, derived from the 1D model results of all the periods.

The cumulate volumes were almost the same whatever the analysed series, changing within the range of $23-29\times10^6$ ton, whereas the resulting effective discharge intervals (Q_{eff} in Table 2), corresponding to the classes with the two larger sediment volumes, were quite different. The distribution in Figure 7 for the twentieth century does not present a very high maximum, and the corresponding Q_{eff} may be detected in the interval of 12,700–16,400 m^3/s. When comparing these values to more detailed data reported in Castro *et al*. (2007), the different time scale and space resolution must be considered. In fact, the 1D model simulates yearly average values for a synthetic description of the river morphology whereas observations by Castro *et al*. (2007) likely refers to monthly time series of the hydrology and topographic survey of specific cross-sections. In that regard, as instance, the yearly averaging applied to the twentieth-century monthly values reduced the range of simulated

Table 2 Time averaged deposition − erosion rate from the 2D model and effective discharge interval, Q_{eff}, and its variability, $\sigma\, Q_{\text{eff}}$ (from the 1D model result analysis over different periods).

Scenario	Deposition (10^6 t/year)	Erosion (10^6 t/year)	Q_{eff} (m^3/s)	$\sigma\, Q_{\text{eff}}$ (m^3/s)
Twentieth century	–	–	**12,700**–16,400	2600
PROMES				
1991–2098	–	–	**17,000**–18,900	1500
2010–2038	6.5	17.4	**17,200**–20,800	1700
RCA				
1981–2100	–	–	17,000–**21,100**	2500
2010–2038	6.6	6.1	14,800–**20,700**	2800
LMDZ				
1991–2048; 2071–2100	–	–	**14,800**–18,900	5500
2010–2038	6.0	8.6	**13,600**–17,500	3900
RegCM3				
1981–2048; 2071–2090	–	–	**18,900**–20,600	1200
2010–2038	8.8	10.2	**17,700**–21,400	1500

Note: The values corresponding to the maximum volume of sediments are given in bold.

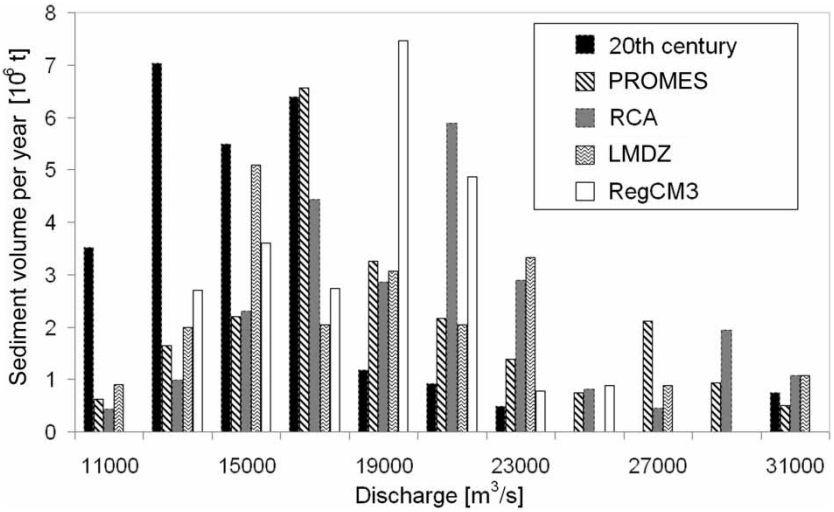

Figure 7 Transported sediment volume over corresponding discharge classes from 1D model results at the Lower Parana.

discharge from 5000–40,000 to 11,000–30,000 m^3/s. This explains the lower effective discharges with respect to Castro *et al*. (2007) values that are within 17,500–20,500 m^3/s in the period from 1900 to 2005.

The variability of each distribution in Figure 7, also reported in Table 2, was assessed as the standard deviation of the classes that cumulate the larger volumes up to about 50% of the total.

The distributions of PROMES and RegCM3 present a single peak, and the other classes are associated to lower volumes, with a hump-shape; on the contrary, the RCA and the LMDZ histograms have a double peak with a bimodal trend. These differences are reflected by assessed variabilities and intervals of the effective discharge: the PROMES and RegCM3 scenarios presented relatively small standard deviations, i.e. less that the 10% of the corresponding effective discharge, while the RCA and LMDZ data were characterized by a great variance, near 20% and 30% of Q_{eff}, respectively. Described differences are related to the distributions of discharge predicted by the applied RCMs (Figure 5(a) and 5(b)).

4.3 *2D morphodynamic simulations*

The four climate scenarios were simulated spanning the period 2010–2038. Each is a combination of different climate models as described in Subsection 3.1 that gave rise to different inflows to the applied 1D model, which in turn provided boundary conditions for the 2D simulations. These conditions were the water-sediment discharge and active channel width at the upstream boundary (Figure 6(a)), and water level at the downstream end (Figure 6(b)). Given the 2D model limitation in representing changing morphology near the boundaries, the computational domain was about extended 10 km upstream and downstream.

Regarding the upstream boundary, the cross-section width variation with discharge was simulated by gathering the inflow discharge in three adjacent threads from the right bank to the left side at floodplain. In more detail and in agreement with 1D model results (Figure 6(a)), the upstream boundary was defined as follows: discharge lower than 20,000 m^3/s flowed into a 2000 m-wide channel at the right bank; the excess in a maximal measure of 5000 m^3/s was conveyed into the adjacent 700 m-wide thread and the remaining part flowed into an additional cross-section portion of 2000 meters. The inflow sediment concentration was maintained homogeneous along the three adjacent threads.

Given the conspicuous increase of the effective discharge for the scenarios in relation to the twentieth century (see Figure 7) the outflow at the downstream boundary was conveyed by means of two threads: the channel at the right bank and the left channel at the floodplain side, which also correspond to the observed margins in 1954.

The model parameters were fixed at simulation 9 values on the basis of the analysis performed on the morphologic sensitivity (Table 1). Consistent with the objective to simulate the observed climate interdecadal variability, yearly averaged values from the 1D model were forced at boundaries; hence, the 2D morphodynamics was simulated with a quasi-steady approach spanning the 29 years of the period 2010–2038.

Figure 8 reports the bed-level total changes as simulated for the four scenarios. Given the inherit inaccuracies from operated oversimplifications, regarding the morphodynamics at boundaries, the lateral erosion and the flow-resistance representations, the resulting bed-level changes are presented in three classes in Figure 8: (1) stable morphology and (2–3) erosion − deposition, for changes within and larger than two meters, respectively, in absolute value and in 29 years. Maximum erosions − depositions were around 10 meters at simulations' end. Two main bar positions are also pointed out in Figure 8 that mostly correspond to bars current positions. During the past 50 years, these bars have progressively diverted water flowing from the meandering sub-sections at the floodplain side to the straight main channel at the river right bank.

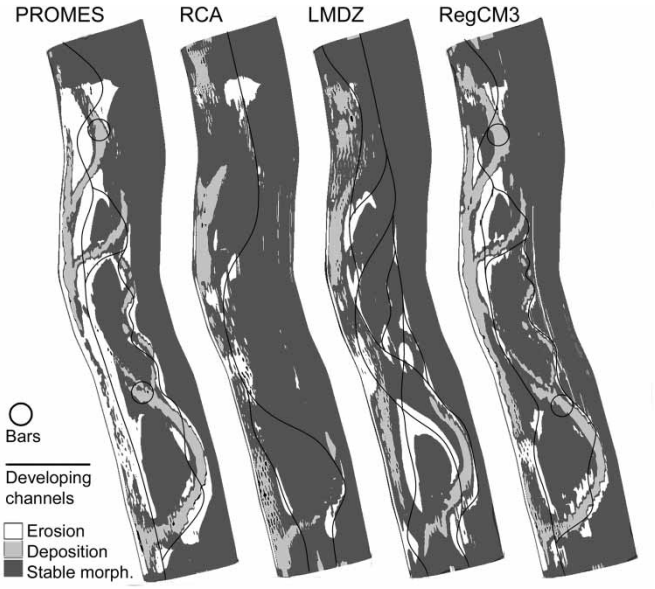

Figure 8 Bed-level total changes from 2010 to 2038 for the four simulated scenarios, with predicted major morphological features.

The most recent margins in Figure 3 from cross-section 1 to 18 mostly correspond to the margins of the bathymetry surveyed in 2009 (Guerrero and Lamberti 2013) which were used to reconstruct the initial morphology. On the basis of 2009 margins and bathymetry, and given the three classes of simulated bed-level changes, channel main threads were superimposed in Figure 8. These threads point out future tendencies of stable-developing channels for the simulated scenarios.

The PROMES and RegCM3 scenarios, but the latter at a lower degree, predicted the main channel widening and consequent streamflow gathering to the right side, and, at the same time, the flux diverting by main bars from meandering channels. Thus, the morphology oversimplification observed during the last 50 years (Castro *et al*. 2007) is kept by these scenarios.

More complex threads were pointed out by RCA and LMDZ simulations: in these cases the meandered channels at the floodplains side appear quite stable whereas depositions follow in the actual main channel at the river right side. In addition, the LMDZ scenario presented jeopardized erosions at islands between actual channels that may yield to a braided morphology.

5 Discussion

Aiming to simulate future tendency in the long-term morphodynamics of the Parana River the applied models introduce relevant simplifications. First, the four climate scenarios presented conspicuous variabilities and deviations among them, probably due to the differences in the physical schemes used to parameterize specific processes (e.g. cloud formation, convection, turbulence) and in the variations arising from the different GCMs used to force them (Saurral *et al*. 2013). In addition, few data (e.g. channel margins) about the past morphology were the only available for implementing-calibrating the morphodynamic models. In 2D models, accurate bathymetries and digital terrain models (DTM) are usually implemented with resolutions in the order of the computational mesh size which can be achieved by means of sonar devices (Guerrero *et al*. 2013) and the Lidar (Williams *et al*. 2011), respectively. Also, limitations in representing lateral erosion and the morphodynamics at boundaries concurred in lowering final result accuracy.

On the other hand, the operated simplifications by the 1D and 2D schemes, also regarding the Local Uniform Flow hypothesis and the quasi-steady approach, respectively, appropriately fit with available data and are needed to predict future long-term tendencies in large river morphodynamics; in fact, given the computational effort, full dynamic 3D codes are unfeasible in such cases.

Given the climate scenarios, the results' reliability mainly depends on the applicability extent of the performed calibrations. The width − discharge relation of the active channel and the flow-resistance law for 1D and 2D models, respectively, appeared particularly relevant in producing the final morphologies. In the 1D model, the statistical distribution of the river width correlated to the corresponding statistical distribution of the flow discharge was adjusted on the basis of various satellite images taken during the period 2000–2010 by means of a calibration procedure reported in Nones (2011). A power law was assumed to map in the 2D model the flow-resistance variation with water-depth accounting of the performed sensitivity analysis on the resulting morphology and of the bedforms-flow velocity investigation reported in Guerrero and Lamberti (2013). Both the width − discharge relation and the flow-resistance law are aimed to account for the lateral erosions at island margins and river shore lines finally affecting the resulting morphology (Cardini *et al*. 2009). In fact, the applied models do not directly simulate the failure mechanism of river margins, but indirectly account of lateral erosion rate which was calibrated by means of the applied width − discharge relation and flow-resistance law in the 1D and 2D models, respectively.

Notwithstanding the encountered limitations, the 1D and 2D models are consistent in pointing out the morphodynamics sensitivity to the simulated discharge distributions. Table 2 reports the effective discharge interval, Q_{eff}, and the corresponding variability, σQ_{eff}, assessed from 1D model results (as described in Subsection 4.2) for all the periods and for the 29-year period of the 2D simulations. Figure 7 shows the corresponding distributions for the longer periods. For the four scenarios, Table 2 also reports the difference between initial and 2D-simulated bathymetry in terms of time-averaged deposition and erosion rate for the entire computational domain, i.e. the integrals of Figure 7 classes over the 29-year period.

Channel-predicted threads from the 2D model (Figure 8) appear correlated to effective discharge values inferred from the 1D model results (Figure 7). Especially when considering maximum values in Table 2, all the four scenarios predicted

pretty high effective discharges with respect to the simulated values for the twentieth century. Different effects arose on the resulting morphology depending on the corresponding discharge distribution. Distributions characterized with lower variability (σ Q_{eff}) yielded a well-developed straight channel at the river right bank, while the meandering channels at the floodplain side was progressively obstructed with bars (PROMES and RegCM3 in Figure 8). This tendency was observed during the twentieth century, which was well characterized by increasing yearly averaged discharges up to maximum values of about 16,000 m^3/s (Table 2). The existing meandering channels appeared more stable for the effective discharge with the largest maximum (RCA result in Figure 8), and the largest discharge variability (σ Q_{eff}) of the LMDZ scenario gave rise to a multi-thread morphology.

Deposition and erosion values in Table 2 reflect the obtained morphologies for the simulated scenarios; in fact eroded volumes were mostly located at the straight channel and were larger for distributions characterized by lower variability, which means the effective discharge was well detected around the maximum sediment volume (i.e. PROMES and RegCM3 in Table 2). The RCA and LMDZ scenarios presented larger variability corresponding to noticeable oscillation of the effective discharge within the simulated period that yielded a deposition at the straight channel and therefore to smaller eroded volume in total.

In general, all the scenarios presented an overall balance between sedimentation and erosion from both 1D and 2D model simulations; as a matter of fact the net sedimentation, i.e. deposition minus erosion in Table 2, is in the order of few percentages of the sediments transported in total.

The 2D model fixed the Lower Parana morphology sensitivity to future scenarios in terms of the corresponding effective discharge distribution assessed over yearly averaged values. Albeit the overall equilibrium that was also reflected in the stability of the river-bed profile (1D model), slight changes of the erosion − deposition balance in Table 2 corresponded to pretty different final morphologies, which appeared mostly correlated to the effective discharge variability. In particular, low variability of the effective discharge changing around 17,000–18,000 m^3/s gave rise to oversimplification of the morphology into a single straight and deep channel (Figure 2), whereas the meandering channel and multi-thread morphology corresponded to a larger variability of the effective discharge changing within the 14,000–21,000 m^3/s interval. This larger variability reflects the discharge oscillation predicted by the corresponding two climate scenarios which noticeably deviates from the past century time series of yearly averaged flow discharge.

6 Conclusions

The application of various models was useful to analyse the Parana River evolution at different spatial and temporal scales: a 1D model was used to simulate the modification of sediment transport rate and the corresponding bed profile dynamics in the longitudinal direction, while the streamflow divagation and the consequent active channel morphodynamics were studied with higher resolution by means of a 2D model.

Despite all the four scenarios applied in this study agreeing on the prediction of an increase in the discharge that most affect the morphology (i.e. the effective discharge), the corresponding distributions are quite different. This variation significantly altered the active-channel morphology (2D model), while the longitudinal bed profile (1D model) was not particularly influenced.

The 1D simulations of past century hydrology and future scenarios show that the bed profile is stable in the longitudinal direction at the scale of the applied model (i.e. morphological box of 80-km length). The Parana River transport capacity result chiefly correlated to flow discharge variation; the longitudinal slope of bed profile being almost the same during simulations, of the order of 10^{-5}.

The channel morphology sensitivity to future scenarios was inferred from 2D simulations of the 2010–2038 period at the 25-km-long section of the Lower Parana. Discharge distributions of different scenarios yielded important modifications to the planimetric morphology. Two scenarios characterized with smaller variability of the effective discharge (assessed over yearly averaged values) changing around 17,000–18,000 m^3/s gave rise to flow gathering into a deep and straight single channel, which is similar to observed oversimplification during the twentieth century. The increased variability of the other two scenarios, reflecting the effective discharge oscillation within the 14,000–21,000 m^3/s interval, appeared effective in forming a multi-thread morphology. The low variability scenarios are more similar to past century time series in terms of flow discharge.

The analysis of the morphological sensitivity to 2D model parameters pointed out the weight of the flow-resistance parameter distribution at the active channel, the floodplains and the islands. In fact, performed simulations of past century morphodynamics gave rise to pretty different morphologies, mainly depending on the assumed variation for roughness parameter passing from the channels to the low-depth areas around margins. A Chézy parameter variation within six times, i.e. from 10 to 60 $m^{1/2}/s$, appeared better consistent with the observed process of the Island Carlota formation near Rosario. This variation affected the simulated lateral erosions at island margins and river shore lines which finally affected the resulting morphology. In fact, the 2D model applied does not directly simulate the failure mechanism of river margins, but indirectly accounts for lateral erosion rate, which was calibrated by means of the applied flow-resistance law.

Given these major results, future studies may address in more detail the reciprocal feedback between margin failure and river channel morphodynamics at the Parana River in light of climate variability. In fact, given the observed morphological sensitivity to simulated lateral erosion, a direct simulation of

margin failure appears to be relevant, which could be coupled to river channel morphodynamics at the time scale of the interdecadal variability.

Acknowledgements

This research has received funding from the European Community's Seventh Framework Programme (FP7/2007–2013) under Grant Agreement No. 212492 (CLARIS-LPB. A Europe-South America Network for Climate Change Assessment and Impact Studies in La Plata Basin).

References

Amsler, M.L., Ramonell, C.G., and Toniolo, H.A., 2005. Morphologic changes in the Paraná River channel (Argentina) in the light of the climate variability during the 20th century. *Geomorphology*, 70 (3), 257–278.

Amsler, M.L., Drago, E.C., and Paira, A.R., 2007. Fluvial sediments: main channel and floodplain interrelationship. *In*: M.H. Iriondo, J.C. Paggi and M.J. Parma, eds. *The Middle Paranà River: Limnology of a subtropical Wetland*. Berlin, Heidelberg: Springler-Verlag, 123–142.

Biedenharn, D.S., *et al.*, 1999. *A practical guide to effective discharge calculation (Appendix A)*. Vicksburg, MS: U.S. Army Corps of Eng.

Cardini, J.C., *et al*., 2009. Desarrollo de una erosión extraordinaria en la margen del río Paraná en Lavalle. Proceedings of *Cuarto Simposio Regional sobre Hidráulica de Ríos*, Salta, Argentina, 2009. in Spanish.

Castro, S.L., *et al*., 2007. Evolución morfológica histórica del cauce del río Paranà en torno a Rosario (km 456–406), *CONAGUA 2007*, Argentina. in Spanish.

DHI Water & Environment, 2002. Mike21C river hydrodynamics and morphology user guide. *DHI*, Horsholm, Denmark.

Di Silvio, G. and Peviani, M., 1989. Modelling Short- and Long-Term evolution of mountain rivers: an application to the torrent Mallero (Italy). *In*: A. Armanini and G. Di Silvio, eds. *Lecture notes in earth sciences*, 37, Fluvial Hydraulics of Mountain Regions, Springer Verlag, 1991, 293–315.

Distributed Archive Data Center, 2000. Global soil data products (IGBP-DIS) [online]. Oak Ridge National Laboratory Distributed Active Archive Center, CD-ROM. Available from: http://daac.ornl.gov/SOILS/guides/igbp.html [Accessed 15 January 2013].

Doyle, M.E. and Barros, V.R., 2011. Attribution of the river flow growth in the Plata Basin. *International Journal of Climatology*, 31 (15), 2234–2248.

Engelund, F. and Hansen, E., 1969. *A monograph on sediment transport in alluvial streams*. Copenhagen, Denmark: Teknisk Vorlag.

Escalante, R., 2008. Estado de Situación de las Vías Navegables. Presented in the workshop *Estudio del Modelo de la Red de Transporte Europeo con El Resto del Mundo – Worldnet*, June 2008. in Spanish.

Fasolato, G., *et al.*, 2011. Validity of uniform flow hypothesis in one-dimensional morphodynamic models. *Journal of Hydraulic Engineering, ASCE*, 37 (2), 183–195.

Garcia, N.O. and Vargas, W.M., 1998. The temporal climatic variability in the Rio de la Plata basin displayed by the river discharges. *Climatic Change*, 38 (3), 359–379.

Garcia, N.O., Vargas, W.M. and Venencio, M., 2002. About of the 1970/71 climatic jump on the Rio de la Plata basin. *Proceedings of the 16th Conference on Hydrology, American Meteorological Society*, 138–141.

Garde, R.J. and Ranga Raju, K.G., 1977. *Mechanism of sediment transportation and alluvial stream problems*. New Delhi, India: Wiley Eastern Ltd.

Guerrero, M. and Lamberti, A., 2012. Flow field and morphology mapping using ADCP and multibeam techniques: Survey in the Po River. *Journal of Hydraulic Engineering, ASCE*, 137 (12), 1576–1587.

Guerrero, M. and Lamberti, A., 2013. Bed-roughness investigation for a 2-D model calibration: the San Martìn case study at Lower Paranà. *International Journal of Sediment Research*, special issue *Sediment loads and processes in large rivers*.

Guerrero, M., Szupiany, R.N., and Amsler, M., 2011. Comparison of acoustic backscattering techniques for suspended sediments investigations. *Flow Measurements and Instrumentation*, 22 (5), 392–401.

Guerrero, M., Ruther, N., and Szupiany, R., 2012. Laboratory validation of ADCP techniques for suspended sediments investigation. *Flow Measurements and Instrumentation*, 23 (1), 40–48.

Guerrero, M., Di Federico, V., and Lamberti, A., 2013. Calibration of a 2-D morphodynamic model using water–sediment flux maps derived from an ADCP recording. *Journal of Hydroinformatics*, 15 (3), 813–828.

Hansen, M., *et al.*, 2000. Global land cover classification at 1 km resolution using a classification tree approach. *Int. J. Remote Sens.*, 21 (6–7), 1331–1364.

Hastings, D.A., *et al*., 1999. The global land one-kilometer base elevation (GLOBE) digital elevation model, Version 1.0 [online]. National Oceanic and Atmospheric Administration, National Geophysical Data Center, 325 Broadway, CO. Available from: http://www.ngdc.noaa.gov/mgg/topo/globe.html

Liang, X., *et al.*, 1994. A simple hydrologically based model of land surface water and energy fluxes for GSMs. *J. Geophys. Res.*, 99 (D7), 14415–14428.

Liang, X., Lettenmaier, D., and Wood, E., 1996. One-dimensional statistical dynamic representation of subgrid spatial variability of precipitation in the two-layer Variable Infiltration Capacity model. *J. Geophys. Res.*, 101 (D16), 21403–21422.

Maciel, F., Díaz, A. and Terra, R., 2010. Variabilidad multi-anual de caudales en ríos de La Cuenca del Plata. Proceedings of the IAHR-AIIH, *XXIV Congreso Latino Americano de hidráulica*, Punta del Este, Uruguay, November 2010. in Spanish.

Montroull, N., *et al*., 2012. Escenarios hidrológicos futuros en la región de los Esteros del Iberá en el contexto del cambio climático. In press in *Meteorológica*. in Spanish.

Nijssen, B., *et al.*, 1997. Streamflow simulation for continental-scale river basins. *Water Resource Research*, 33 (4), 711–724.

Nones, M., 2011. *Aspects of riverine hydro-morpho-biodynamics at watershed scale* [online]. Thesis (PhD). University of Padua, Italy. Available from: http://paduaresearch.cab.unipd.it/4468 [Accessed 15 January 2013].

Nones, M., Guerrero, M. and Gaeta, M.G., 2012. Analysis of the 1-D morphological evolution of the Paranà River. Submitted to *Journal of Hydraulic Engineering*.

Olesen, K.W., 1987. Bed topography in shallow river bends. Delft: Faculty of Civil Engineering.

Saurral, R., 2010. The hydrologic cycle of the La Plata Basin in the WCRP-CMIP3 multimodel dataset. *Journal of Hydrometeorology*, 11 (5), 1083–1102.

Saurral, R., Montroull, N. and Camilloni, I., 2013. Development of statistically unbiased 21st century hydrology scenarios over La Plata Basin, *International Journal of River Basin Management*, special issue *Impact Assessment of Climate Change on La Plata Basin Water Resources*.

Su, F. and Lettenmaier, D., 2009. Estimation of surface water budget of La Plata Basin. *Journal of Hydrometeorology*, 10 (4), 981–998.

Talmon, A. M., 1992. *Bed topography of river bends with suspended sediment transport*. Thesis (PhD). Delft Univ. of Technology, The Netherlands.

Williams, R.D., *et al.*, 2011. Monitoring braided river change using terrestrial laser scanning and optical bathymetric mapping. *In*: M. Smith, P. Paron and J. Griffiths, eds. *Geomorphological mapping: methods and applications*. Amsterdam: Elsevier, 507–532. doi:10.1016/B978-0-444-53446-0.00020-3. [Accessed 15 January 2013].